RSC Advances

ROYAL SOCIETY OF CHEMISTRY

www.rsc.org/advances

Response surface optimization and Artificial neural network modeling of biodiesel production from crude Mahua (*Madhuca indica*) oil under supercritical ethanol condition using CO_2 as co-solvent

Antaram Sarve*, Mahesh N. Varma, Shriram S. Sonawane

Department of Chemical Engineering, Visvesvaraya National Institute of Technology (VNIT), South Ambazari Road, Nagpur (M.H.) 440010, India

*** Corresponding author:**

A. N. Sarve

Department of Chemical Engineering, Visvesvaraya National Institute of Technology (VNIT), South Ambazari Road, Nagpur (M.H.) 440010, India

E-mail address: anant4u87@gmail.com

Phone No: 07122801646

Abstract

The present study describes the renewable, environment-friendly approach for the production of biodiesel from low cost, high acid value mahua oil under supercritical ethanol condition using carbon dioxide (CO_2) as a co-solvent. CO_2 was employed to decrease the supercritical temperature and pressure of ethanol. Response surface method (RSM) is the most preferred method for optimization of biodiesel so far. In last decade, artificial neural network (ANN) has come up as one of the most efficient method for empirical modeling and optimization, especially for non-linear systems. This paper presents the comparative studies between RSM and ANN for their predictive, generalization capabilities, parametric effects and sensitivity analysis. Experimental data were evaluated by applying RSM integrating with desirability function approach. The importance of each independent variable on the response was investigated by using sensitivity analysis. The optimum conditions were found to be temperature (304 ^{o}C), ethanol to oil molar ratio (29:1), reaction time (36 min), and initial CO_2 pressure (40 bar). For these conditions, experimental fatty acid ethyl ester (FAEE) content of 97.42% was obtained, which was in reasonable agreement with predicted one. The sensitivity analysis confirmed that temperature was the main factors affecting the FAEE content with the relative importance of 39.24%. The lower values of correlation coefficient (R^2 =0.868), root mean square error (RMSE =4.185), standard error of prediction (SEP =5.81) and absolute average deviation (AAD =5.239) for ANN compared to those R^2 (0.658), RMSE (7.691), SEP (10.67) and AAD (8.574) for RSM proved better prediction capability of ANN in predicting the FAEE content.

Keywords: Mahua oil, Supercritical ethanol, Biodiesel, Response surface method, Artificial neural network

1. Introduction

To solve the problems of global warming, fluctuating oil prices, CO_2 emissions, and possibly create new job opportunities, extensive research and development programs are in search of renewable energy sources are actively pursued. Biofuels have become an important renewable energy source, particularly for the transportation applications. As a renewable energy source, biomass is one of the superior sources of energy and industrial-scale biomass based energy production could improve the socioeconomics of many underdeveloped societies and countries along with the raising awareness of environmental protection. [1] Biodiesel composed of mixture of alkyl esters that mostly produced by esterification and transesterification of various lipid feedstocks such as vegetable oils and animal fats with methanol or ethanol as the reacting alcohol. [2] One of the major problems for the use of biodiesel is the poor availability the economic raw material. Therefore, different alternative feedstocks for biodiesel production need to be explored. In India, with abundance of forest resources, there are number of non-edible tree borne oilseeds with an estimated annual production of more than 20 million tones, which have great potential for making biodiesel to supplement other conventional sources. Among the available feedstocks, mahua (*Madhuca indica*) is an economically important oilseed tree of the Sapotaceae family, which grows in several parts of India. Mahua (*Madhuca indica*) is one such non-edible tree based seed oil, which has an estimated annual production potential of 181,000 Mt in India. [3] Fatty acid composition of mahua oil has earlier been reported in literature [4,5] and is given in Table S1. The major constituents are palmatic, stearic, oleic, linoleic, arachidic which contribute about 96% of total fatty acids present in mahua oil.

The studies about biodiesel production from mahua oil via alkali catalysed transesterification have been reported in the literatures. [5,6] Kumari et al. [4] employed lipase catalyst (*Pseudomonas cepacia immobilized on CLEAs and PCMCs*) for synthesis of biodiesel from mahua oil with high free fatty acid content (20%) and reported 92 % conversion in 2.5 h with (cross-linked enzyme aggregates) CLEAs, 99% conversion in 2.5 h with (protein-coated microcrystals) PCMCs. However, the catalytic biodiesel production has several drawbacks such as time-consuming due to low reaction rate and corrosion risk for acid-catalyzed, high sensitivity to free fatty acid (FFA) and water contents in the oil feedstock and difficulty in the separation of biodiesel and catalyst from soap for alkaline catalyst, high cost and deactivation risk of the active sites for both enzyme and heterogeneous catalysts. Moreover, biodiesel production employing

liquid catalysts requires complex and costly treatments for the acidic or alkaline wastewater.[2] Recently, supercritical transesterification (SC-TE) has been highlighted as an emerging technology for the biodiesel synthesis from various feedstocks. This method is able to completely convert fatty acids in feedstocks to alkyl ester with high purity without involving any catalysts and offers simple product separation from the mixture. [7] Other advantages of this route include fast reaction kinetics, ease separation of products, and tolerance to FFA and water contents in the oil feedstock because esterification of free fatty acid (FFA) and transesterification of triglycerides proceed simultaneously. [2] Apart from the advantages, it has some drawbacks like high equipment cost and high energy consumption due to high temperature and pressure conditions. This limits the supercritical transesterification process to be viable for large scale industrial applications. However, the introduction of co-solvents like hexane, carbon dioxide, propane into the reaction mixture decreases the severity of the reaction parameters and can make this process practical. The addition of co-solvents can decrease the critical point of alcohol and allow the supercritical reactions to be carried out at milder temperatures. [8] Different alcohols such as methanol, ethanol, propanol, butanol and amyl alcohol can be used for the transesterification. Ethanol is preferred in present study because it is renewable, non-toxic, eco-friendly and can be produced from agricultural resources. Also, fatty acid ethyl ester are better than fatty acid methyl esters in term of fuel properties, including cetane number, oxidation stability and cold flow properties. [1]

In the last decades the different mathematical tools, useful for modeling and optimization of biodiesel synthesis, have been progressively developed. For instance, response surface methodology (RSM) and artificial neural networks (ANN) are powerful mathematical methods suitable for modeling and simulation of various processes in real applications. Both methodologies do not need the explicit expressions of the physical meaning of the system or process under investigation. Therefore, RSM as well as ANN belong to modeling techniques dealing with the development of non-parametric simulative models. Such models have a wide applicability in various disciplines of science. In fact, these models approximate the functional relationships between input variables and the output (response) of the process using experimental data. Afterwards, the models are used to estimate the optimal settings of input variables to maximize or minimize the response. [9]

Biodiesel production has been predicted and optimized using several topologies of ANN in a few studies. [10-14] Yuste and Dorado, [12] accurately simulated base-catalyzed waste olive oil transesterification for biodiesel production using an ANN model introducing a tool for making a decision in the experimental process. They showed that the ANN is a capable alternative tool for experimentally testing of the process optimization. Ramadhas et al. [15] developed different ANN models based on multi-layer feed forward, radial base, generalized regression and recurrent network for predicting the cetane number (CN) of biodiesel fuel. The predicted CN of biodiesel is comparable to that of actual CN of the biodiesel. Rodríguez et al. [16] applied multiple linear regression and artificial neural networks for obtaining a model for predicting cetane number and validated the model using data from literature. The models based on multiple linear regressions cannot predict cetane number with similar accuracy as the obtained for the selected neural network. The biodiesel production from rapeseed soapstock and methanol in the presence of the *candida-rugosa* lipase immobilized on chitosan was analyzed by Ying et al. [17] using an ANN, showing desirable correspondence between predicted and experimental values of the FAME yield. Basri et al. [18] has reported the comparison of ANN and RSM in lipase-catalyzed synthesis of palm-based wax ester, which also suggest the superiority of ANN over RSM for both data fitting and estimation capabilities.

RSM and ANN have been widely applied for the modeling and optimization of biodiesel synthesis from various feedstocks using different methods such as classical base catalyzed transesterification, [13,14,19,20] heterogeneous base catalyzed transesterification, [21] conventional two-step acid catalyzed esterification and base catalyzed transesterification, [22,23] ultrasound assisted base catalyzed transesterification, [24] ultrasound assisted two-step acid catalyzed esterification and base catalyzed transesterification, [25,26] ultrasound assisted heterogeneous base catalyzed, [27] lipase catalyzed, [18] Infrared irradiation assisted esterification,[28]. Several papers took advantages of the genetic algorithm coupled with ANN to generate optimum operating variables for the studied process. [11,17, 22] Most of the reported literatures on comparison of RSM and ANN for biodiesel synthesis using different feedstocks were based on conventional, ultrasound, and infrared irradiation assisted techniques. To the best of our knowledge, there are no studies dealing with comparison of RSM and ANN modeling methods for the optimization of non-catalyzed biodiesel synthesis using non-edible oil.

Hence, the objective of the present work is to demonstrate the conversion of high free acid content crude mahua oil into biodiesel using single step supercritical ethanol process in presence of carbon dioxide (CO_2). In order to assess and understand the effect of each variable on fatty acid ethyl ester (FAEE) content, statistical analysis was performed using the RSM. Moreover, the desirability function approach for optimization of FAEE content was employed in order to develop an efficient method for achieving maximum biodiesel production. In addition, the present work investigates the predictive and generalization capability of artificial neural network (ANN) to estimate the FAEE content. Furthermore, the efficiencies of both the models were statistically compared by the coefficient of determination (R^2), root mean square error (RMSE), standard error of prediction (SEP), and absolute average deviation (AAD) based on the validation data set.

2. Experimental Section

2.1. Materials

Mahua oil was obtained from local market. Anhydrous ethanol (99.8%) was purchased from Mars scientific Inc. (Australia). Carbon dioxide (99%) was supplied by Bharti Gases (Nagpur, India). All chemicals including n-hexane (95%) and Sulfuric acid (99%) of analytical reagent (AR) grade was purchased from Merck Limited, Mumbai, India. Hexanoic acid (S.D. Fine Chem. Ltd. India) was used as an internal standard for the gas chromatographic analyses. The standards required for quantification of esters were procured from Sigma-Aldrich Co. Ltd., Mumbai, India and were chromatographically pure. All the liquid chemicals were filtered through 2 μm pore size filter and the gases were passed through silica bed prior to use.

The acid value of oil was determined by acid base titration technique, [29] using the standard solution of KOH. Mahua oil had an initial acid value of 36 mg of KOH/g of oil. The critical temperature and pressure of ethanol is 516.2 K and 6.4 MPa. The properties of the ethanol favor the homogeneous mixing with oil at supercritical condition because they act as acid catalysts in the supercritical biodiesel synthesis. [30]

2.2. Methods

The supercritical ethanol process was carried out in a 50mL bench top AMAR 2630 high pressure reactor (SS 316) equipped with a E-3032 controller, magnetic stirrer, pressure gauge, external electric heater (Amar Equipments Pvt. Ltd., Mumbai, India). The instrument can be operated maximum up to 500 ^{o}C and 400 bars. The complete experimental set-up has been

shown in Fig. S1. A known amount of mahua oil and ethanol was charged to the reactor to give the different amount of ethanol to oil molar ratio ranging from 15:1 to 35:1. The reactor was then purged with known amount of CO_2 gas (10 - 50 bars) as co-solvent. Then, the mixture of mahua oil-ethanol-CO_2 was heated at the different temperatures (250 ^oC - 350 ^oC) for which the power was adjusted to give a heating rate 50 ^oC/ min and is defined as the zero reaction time (temperature and pressure reached the set value). The temperature was controlled within ± 2 ^oC and the pressure was monitored by pressure gauge in order to maintained the isothermal and isobar reaction conditions. After the set value reached, the mixture was stirred with magnetic stirrer for desired time (10 - 50 min). To stop the reaction after the predetermined reaction time, the reactor was quenched by immersing the reactor in a cold water bath. The product was collected, and hexane was used to elute any trace of product left in the reactor. The alcohol and hexane present with product was evaporated at 90 °C, leaving behind the mixture of unreacted oil, ester, and glycerol, and then taken for analysis by gas chromatography.

2.3. GC Analysis

The reaction samples were analyzed by gas chromatography (model GC-2010 plus, Shimadzu Corp., Tokyo, Japan) using a capillary column, MXT-Biodiesel TG (Restek, USA; 15 m × 0.32 mm × 1μm film thickness of diphenyl dimethyl polysiloxane) and a flame ionization detector. Nitrogen was used as a carrier gas at a flow rate of 2.75 mL min^{-1}. Hexanoic acid was used as an internal standard. Column oven temperature was initially maintained at 100 ^oC for 3 minutes, then increases to 250 ^oC at the rate of 30 ^oC min^{-1} and held here for 3 minutes. The injector and detector temperature were maintained at 270 ^oC. A sample volume of 1 μL mahua oil biodiesel (MOB) in hexane was injected using a split mode, with the split ratio of 1:50. The GC chromatograph of MOB is shown in Fig. S2.

2.4. Experimental Design

2.4.1. Response surface method

A five-level four-factor central composite experimental design (CCD) was used in this study. Reaction temperature (A), ethanol to oil molar ratio (B), time (C), and initial CO_2 pressure (D) were the input variables, the factor levels were coded as -2 to +2 as shown in Table S2. In this work, the input variables (factors) and their levels were selected, based on preliminary experiments carried out in the laboratory. According to the CCD, experiments were performed in order to find out the optimum combination and study the effect of process parameters on FAEE

content using the supercritical ethanol (SC-ET) process, and the results are given in Table 1. Experimental data from the CCD was analysed using regression (Design Expert ™ 8.0) and fitted to a second-order polynomial model in order to identify all possible interactions of selected factors with response function as follows:

$$Y = b_0 + \sum_{i=1}^{k} b_i\ x_i + \sum_{i=1}^{k} b_{ii}\ x_i^2 + \sum_{i=1}^{k}\sum_{i=j}^{k} b_{ij}\ x_i x_j + e \quad (1)$$

where, Y is response (FAEE content %), b_0, b_i, b_{ii} and b_{ij} are the regression coefficients obtained for constant, linear, quadratic and interaction terms, respectively. x_i and x_j are independent variables, whereas i and j are the linear and quadratic coefficients, respectively. b is the regression coefficient, k is the number of factors studies and optimized in the experiment and e is random error. Furthermore, RSM integrated with desirability function approach was used for simultaneous optimization of FAEE content.

2.4.2. Desirability function approach

The individual desirability (d) for response was calculated by one side transformation method (Eq. 2), followed by calculation of overall desirability (D) using univariate technique (Eq. 3) as follows: [27,31,32]

$$d_i = \begin{cases} 0 & Y_i \le Y_{i-min} \\ \left[\frac{Y_i - Y_{i-min}}{Y_{i-max} - Y_{i-min}}\right]^r & Y_{i-min} < Y_i < Y_{i-max} \\ 0 & Y_i \ge Y_{i-max} \end{cases} \quad (2)$$

$$D = (d_1^{w1} d_2^{w2} d_3^{w3} d_4^{w4} d_5^{wn})^{1/\sum w_i} \quad (3)$$

where d_i is individual response desirability, Y_i is the response values, $Y_{i\text{-}min}$ is the minimum acceptable value for response i, $Y_{i\text{-}max}$ is the maximum acceptable value for response i, r is a weight used to determine the scale of desirability, D is the overall desirability, d_i is individual response desirability, and w_i is a weighted composite desirability.

2.4.3. Artificial neural network

The design of experiments (DoE), which is used for training the network and respective experimental response (FAEE content) are given in Table 1. In this work, the network inputs and target have been normalized before training. To this end, both input variables and target (experimental response) have been normalized ranging from -1 (minimum level) up to +1 (maximum level). The normalization in the limits (-1,+1) was carried out since the tangent sigmoid function (tansig) employed for ANN modeling ranges from -1 and +1. For normalization target data the following equation was used: [33]

$$\text{Normalized} = \left[\frac{2*(X_{Ac}-X_{min})}{(X_{max}-X_{min})}\right] - 1 \quad (4)$$

where X_{min}, X_{max}, and X_{Ac} are the minimum, maximum and actual data, respectively. The normalization of inputs and target was performed to avoid overflows that may appear due to very large or very small weights. [9] In this study, a three-layered feed-forward neural network with tangent sigmoid transfer function (tansig) at hidden layer and a linear transfer function (purelin) at output layer was used. The sigmoid transfer function was given by (Eq. 5).

$$f(x) = 2 \times \frac{1}{1+e^{-2x}} - 1 \quad (5)$$

and the linear activation function (Eq. 6) is used as the output layer activation function. [34]

$$f(x) = x \quad (6)$$

The back propagation algorithm was used for network training. Sixty percent of the data was taken for the training set, twenty percent for the validation set and rest of the data for the test set. Neural Network Toolbox V4.0 of MATLAB mathematical software was used for FAEE prediction. The performance of ANN was statistically measured by root mean square error (RMSE), standard error of prediction (SEP), absolute average deviation (AAD), and correlation coefficients (R^2) was carried out between experimental and predicted data. The formulas used for error analyses were calculated by Eq. (7) to Eq. (10) respectively. [27,35,36]

$$R^2 = 1 - \frac{\sum_{i=1}^{n}(Y_{i,p}-Y_{i,e})^2}{\sum_{i=1}^{n}(Y_{i,p}-Y_e)^2} \quad (7)$$

$$RMSE = \sqrt{\frac{\sum_{i=1}^{n}(Y_{i,e}-Y_{i,p})^2}{n}} \quad (8)$$

$$SEP = \frac{RMSE}{Y_e} \times 100 \quad (9)$$

$$AAD = \frac{100}{n} \sum_{i=1}^{n} \frac{|(Y_{i,p}-Y_{i,e})|}{|(Y_{i,e})|} \quad (10)$$

where, $Y_{i,e}$ is the experimental data, $Y_{i,p}$ is the corresponding data predicted, Y_e is the mean value of experimental data and n is the number of the experimental data.

2.4.4. Sensitivity Analysis

ANN being a *black box model*, it does not give insights of the system directly. But there are numerous methods available which gives the sensitivity analysis of the system using inherent nature of ANN. In order to evaluate the relative importance of each Input variable on the response, Garson [37] proposed an equation based on the partitioning of the connection of the weights as:

$$I_j = \frac{\sum_{m=1}^{m=N_h}((\left|W_{jm}^{ih}\right|/\sum_{k=1}^{N_i}\left|W_{km}^{ih}\right|)\times|W_{mn}^{ho}|)}{\sum_{k=1}^{k=N_i}\{\sum_{m=1}^{m=N_h}(|W_{km}^{ih}|/\sum_{k=1}^{N_i}|W_{km}^{ih}|)\times|W_{mn}^{ho}|\}} \quad (11)$$

where, I_j is the relative significance of the j^{th} input variable on the output variable, N_i and N_h are the number of input and hidden neurons, respectively. *W* is connection weight, the superscripts *i, h* and *o* represents the input, hidden, and output layers, respectively. while the subscripts *k, m* and *n* refer to input, hidden, and output neurons, respectively. [37]

3. Results & Discussion

3.1. RSM modeling and Desirability function approach for Optimization

The second-order polynomial equation was fitted with the experimental results obtained on the basis of CCD experimental design. The final equation obtained in terms of coded factors as follows:

$$\text{FAEE content (\%)} = 87.82 + 3.02A + 4.73B + 8.26C + 2.05D + 2AB - 1.46AC - 0.038AD + 0.085\,BC - 1.09BD - 0.036CD - 12.58\,A^2 - 4.06B^2 - 6.89C^2 - 0.64D^2 \quad (12)$$

The adequacy and fitness of the model was tested by analysis of variance (ANOVA), which is shown in Table 2. The regression analysis indicates that all the four parameters had significant influence on the fatty acid ethyl ester (FAEE) content, which is confirmed by the *P*-values. The *P*-value of the lack of fit analysis is 0.0825, which is more than the 0.05 (confidence level is 95%). The regression model provides accurate description of the experimental data indicating successful correlation among the four transesterification process parameters that affect the FAEE content. The value of R^2 was calculated to be 0.9709, which indicated good agreement of model value with experiment. The model was then further process to generate response surface plots using Matlab Version 8.3 (R2014a).

3.2. Effect of process parameters

Three-dimensional response surface plots are shown in Figs. 1(a-c) revealing the predicted effects of factors on the response. Fig. 1a shows the influence of reaction temperatures and ethanol/oil molar ratio on FAEE content for fixed levels of reaction time of 30 min and initial CO_2 pressure of 30 bar. Fig. 1a shows that FAEE content increased with the increase in temperature from 275 to 305 ^oC, afterwards the trend is reversed. This may be due to the partial thermal degradation of mono- and polyunsaturated fatty acids present in mahua oil. [38] Imahara et al. [39] reported that unsaturated fatty acids tend to decompose at high temperature and pressure conditions due to the isomerization of double bond functional group from cis-type carbon

bonding into trans type carbon bonding which are naturally unstable fatty acids. Similar observation has been reported by other researchers who investigated the production of biodiesel from wet algal biomass using methanol [40] and ethanol conditions. [1]

Fig. 1a also depicts the effect of the ethanol/oil molar ratio on FAEE content. Stoichiometrically, ethanol to oil molar ratio of 3:1 is required to form three moles of fatty acid ethyl esters (biodiesel) and one mole of glycerol. In supercritical transesterification process, the molar ratio of ethanol to oil used is significantly higher than the stoichiometric amount. This can be explained on the basis that a large excess molar ratio of ethanol to oil is required to bring the reaction system to homogeneous supercritical state. Moreover, a large excess molar ratio of ethanol to oil was purposely used to drive the chemical equilibrium to the right-hand side based on Le Chatelier's principle and ensures high conversion of triglycerides within short time, and also high amount of ethanol act as a solvent, acid catalyst and reactant for oil to ester conversion. The conversion of triglycerides into fatty acid ethyl esters takes place sequentially as follows: (i) the reaction between ethoxide anion and the carbonyl carbon of triglyceride to form ethyl ester and diglyceride; (ii) the reaction between ethoxide anion and the carbonyl carbon of diglyceride to form ethyl ester and monoglycerides; and (iii) the reaction between ethoxide anion and the carbonyl carbon of monoglycerides to form ethyl ester and glycerol. [2,41]

Fig. 1a shows that increase in ethanol to oil molar ratio increases the FAEE content up to 30:1 and further increases in ethanol to oil molar ratio decreases the FAEE content. Initially, the increase in the FAEE content is due to the increased contact area between ethanol and oil and the increased mutual solubility in the presence of co-solvent CO_2. Later, excess ethanol started to interfere with the glycerin separation due to increased solubility, which resulted in lower FAEE content. [8,42] According to He et al. [43], after the mixture of alcohol and oil changes into a homogenous state, continuing raising the molar ratio of alcohol to oil cannot help to increase the fatty acid alkyl ester yield, as the reaction is restrained by the reaction equilibrium, which also makes the increase dosage of alcohol do not lead to any obvious effect on the fatty acid alkyl ester yield after a certain value of the molar ratio. The maximum FAEE content was achieved at temperature of 304 ^{o}C and ethanol to oil molar ratio of 29:1.

Reaction time plays a crucial role in the economy of the process and productivity. Conventional transesterification reactions take hours to complete while supercritical alcohol transesterification can be achieved in much shorter time periods. [1] Balat conducted experiments

under condition 280 ^{o}C, molar ratio of 40:1 of sunflower to ethanol. The fatty acid ester content (FAEE) content was 80% after 300 s. [44] Muppaneni et al. [8] reported 91% of FAEE yield at 300 ^{o}C, 33:1 ethanol to oil molar ratio, and 20 min of reaction time. Fig. 1b shows the influence of reaction temperatures and time on FAEE content for fixed levels of ethanol/oil molar ratio of 25:1 and initial CO_2 pressure of 30 bar. It can be seen from Fig. 1b that reaction time has positive effects on FAEE content up to 36 min, and thereafter it shows negative impacts on FAEE content. The optimal residence time in our experiment was somewhat different from those in other reports, [8,44] which may be explained by the difference between their experimental conditions, and ours as well as varied nature of oil. The major reason for the decrease of the FAEE content after the critical point of residence time at high reaction temperatures is the loss of unsaturated FAEE. In the reaction conditions of high reaction temperatures, namely above 304 ^{o}C, there were other side reactions already, such as thermal decomposition reactions and dehydrogenation reactions [1,40,43,45] consuming the unsaturated FAEE, especially the C18:1 and C18:2. At the beginning of a transesterification reaction, the rate of FAEE production is higher than that of FAEE consumption, and therefore the content of FAEE increases before reaching the equilibrium point between the transesterification reaction and the side reactions. However, after this point, the rate of FAEE consumption is higher than that of FAEE production, and with the increase of residence time, the FAEE decreases.

Fig. 1c shows the effects of temperature and initial CO_2 pressure on FAEE content, when ethanol/oil molar ratio and reaction time were maintained constant as 25:1 and 30 min, respectively. As one can see, with the increment of initial CO_2 pressure up to the level of 40 bar, the FAEE content increases, beyond 40 bar there is no significant effect of initial CO_2 pressure on FAEE content. Han et al. [46], in the alcoholysis of soyabean oil in methanol with the addition of co-solvent CO_2, found that significant decrease in the severity of the process conditions required for supercritical reaction. Yin et al. [47] reported that esters yield for the reaction using supercritical methanol increased when using carbon dioxide as co-solvent. Tsai et al. [48] reported that addition of CO_2 in supercritical transesterification of sunflower oil using methanol is insignificant on FAEE yield at higher pressures above 10 MPa. For stating the significance of CO_2 pressure on the reaction, separate reactions were carried at optimum condition such as by using CO_2 and without using CO_2. The FAEE content observed was 97.42% for CO_2 pressurized reaction and 76.83% for without CO_2. This experiment analysis shows that CO_2 has the

significant effect on reaction kinetics. The possible reason may be the fact that increasing the reaction pressure simultaneously increases the density of the reaction mixture. The transesterification conversion is enhanced with an increased reaction mixture density. [43]

The RSM integrated with desirability function approach was used for simultaneous optimization of FAEE content, owing to its potential over conventional RSM. [27] The global optimized conditions for FAEE content were found to be temperature (A) = 304 ^{o}C, ethanol to oil molar ratio (B) = 29:1, reaction time (C) = 36 min, initial CO_2 pressure (D) = 40 bar. The predicted response of FAEE content at optimized conditions was 95.08 % (wt), with D value of 0.9316. The maximum FAEE content of 97.42% (wt) was obtained at optimized conditions, representing only 2.34% difference between estimated and actual FAEE content. Results suggested that the optimal conditions attained had the least error and can be practically applied to produce biodiesel from mahua oil.

3.3. Artificial Neural Network modeling

The optimum architecture of ANN model was determined based on three steps: (1) optimum number of neurons (2) selection of the best backpropagation training algorithm and (3) testing and validation of the model. [27] A number neural network architecture and topologies were selected and investigated for the estimation and prediction of FAEE content. This is due to the fact that the choice of an optimal neural network and architecture and topology is critical for successful application of ANN. [49]

The optimum number of neurons was determined based on the minimum value of mean square error (MSE) of the training and prediction set. [50] In optimization of the neural network, two neurons were used in hidden layer as an initial estimate. The training stops with MSE of 0.00017 at 48 epoch, which are close to the acceptable limit for MSE to 0.001. The relation between MSE and number of neurons in the hidden layer is given in Fig. S3. As it can be seen, the MSE of was minimum just about 10 neurons. The best backpropagation algorithm was determined by studying ten different backpropagation algorithms using tansig transfer function at hidden layer and purelin transfer function at output layer and results are given in Table 3. Polak-Ribiere conjugate gradient backpropagation (CGPA) with smaller MSE was found to be the best of ten backpropagation algorithms. So, CGPA was considered as the training algorithm in this study. Hence, we used feed-forward CGPA with 10 artificial neurons in hidden layer for modeling of FAEE content. The optimum architecture of ANN (4:10:1) model in this case is

shown in Fig. 2. Fig. 2 consists of three layers as input layer with four input variables, hidden layer with ten hidden neurons, and output layer with single output variable. All neurons from hidden layer have tan-sigmoid transfer function (tansig) and the output layer neuron has linear transfer function (purelin). As can be seen from Fig. 2, the connections consist of weights and biases between inputs and neurons as well as between neurons from different layers.

The scatter diagrams that compare the experimental data versus the computed neural network data in both training, testing and validation networks are shown in Fig. 3. Fig. 3 shows the NN model with training, validation, test and all prediction set with very good values of R (0.9989, 0.9998, 0.9999, and 0.9994 respectively). Almost all data scatter around the 45^{o} line that is the indication of excellent compatibility between the experimental results and ANN predicted data. These values of R between experimental response and ANN predicted response in all the cases suggests that the developed ANN model, which was trained using experimental data, was precise predicting FAEE content.

3.4. Sensitivity Analysis

The ANN used in this study provided with weights listed in Table 4a. The relative significance of the four input variables calculated by Garson Eq. (11) shown in Table 4b. As may be seen from Table 4b, all of the four variables (temperature, ethanol/oil molar ratio, time, and initial CO_2 pressure with relative importance of 39.24, 19.61, 28.57 and 12.58 respectively) have strong effects on the FAEE content. Therefore, none of the variables studied in this work could have been neglected in the present analysis. The degree of effectiveness of variables was found in the order of.

temperature > reaction time > ethanol/oil molar ratio > initial CO_2 pressure

3.5. Comparison between RSM and ANN models

The ANN and RSM model were compared for DoE, using which both the models were trained. The comparison was made on the basis of various parameters such as root mean square error (RMSE), standard error of prediction (SEP), absolute average deviation (AAD), and correlation coefficients (R^2). The predicted values by ANN as well RSM model are tabulated in Table 1. ANN model had fitted the experimental data with an excellent accuracy. The generalization ability of both the models were judged only with unseen dataset. Thus, it was decided to test both the models using the separate unseen data (six runs) which does not belong to the training data sets. The experimental and predicted FAEE content are summarized in Table

5. The comparative values of RMSE, SEP, AAD and R^2 are given in Table 6. The R^2 for RSM and ANN was 0.658 and 0.868, and RMSE was 7.691 and 4.185, respectively. Table 6 indicates that both the models performed reasonably well, but ANN performed consistently better than RSM. The prediction performance of the ANN model for the validation data set confirmed its superior generalization capacity for the given case over the RSM. In addition, Fig. 4 shows the experimental and predicted values for each experimental run to obtained the FAEE content. From the Fig. 4, it is evident that the trained neural network has efficient approximated experimental values. The ANN model predictions lie much closer to the line of perfect prediction than the RSM model. Thus, the ANN model shows a significantly higher generalization capacity than the RSM model. This higher predictive accuracy of the ANN can be attributed to its universal ability to approximate the nonlinearity of the system, whereas the RSM is restricted to a second-order polynomial. [51] However, when using the ANN technique one must have in mind that its predictions are restricted on the process factors inside the ranges applied in the training process. [14]

3.6. Fuel properties of Mahua oil Biodiesel

A comparison of fuel properties are made between mahua oil, mahua oil ethyl ester, ASTM and DIN EN 14214 Biodiesel standard which are given in Table 7. The various properties of mahua oil biodiesel (MOB) are found to be comparable with that of the Diesel, American (ASTM) and Europian (DIN EN 14214) biodiesel standard. Cetane number is high, favorable for combustion. Flash point and Fire point are high, which is an advantage for fuel transportation.

4. Conclusions

The production of biodiesel from crude mahua oil with high content of free fatty acid by ethanolysis reaction at supercritical condition using CO_2 as co-solvent has been investigated in this work. Experimental results demonstrated that use of co-solvent helps to increase FAEE content at lower process conditions, which facilitates less energy consumption for biodiesel conversion. In this work, RSM and ANN were applied for modeling and optimization of the supercritical biodiesel production process. Response surface method (RSM) integrated with desirability function approach was successfully applied for designing and optimizing the experiments with respect to the dependent variables. The regression equations in coded and actual terms were calculated by RSM to describe the empirical functional relationship between input variables and response (FAEE content). The biodiesel was found to content more than 97% FAEE content, which is well above EN 14214 limits of 96.4%. The sensitivity analysis of ANN confirmed that all the four variables have significant effects on FAEE content with the degree of effectiveness in order of temperature > reaction time > ethanol/oil molar ratio > initial CO_2 pressure. Based on the values of R^2, RMSE, SEP, AAD for validation data sets, ANN model was demonstrated to be more efficient than RSM model both in data fitting and prediction capabilities. This renewable, eco-friendly process has the potential to provide a sustainable route for the production of high-quality biodiesel using low cost, high acid value, crude mahua oil. However, further exploration on this technology is necessary for scale up of process design, reaction kinetics and thermodynamics, storage stability, fuel analysis using the biodiesel fuel engine.

Appendix A. Supplementary Material

References

[1] Reddy, H.K.; Muppaneni, T.; Patil, P.D.; Ponnusamy, S.; Cooke.; P.; Schaub, T.; Deng, S. *Fuel* **2014**, *115*, 720-726.

[2] Ong, L.K.; Effendi, C.; Kurniawan, A.; Lin, C.X.; Zhao, X.S. *Energy* **2013**, *57*, 615-623.

[3] Ghadge, S.V.; Raheman, H. *Bioresource Technology* **2006**, *96*, 379-384.

[4] Kumari, V.; Shah, S.; Gupta, M.N. *Energy & Fuels* **2007**, *21*, 368-372.

[5] Ghadge, S.V.; Raheman, H. *Biomass and Bioenergy* **2005**, *28*, 601-605.

[6] Puhan, S.; Vedaraman, N.; Ram, B.V.P.; Sankarnarayanan, G.; Jaychandran, K. *Biomass and Bioenergy* **2005**, *28*, 87-93.

[7] Ong, L.K.; Kurniawan, A.; Suwandi, A.C.; Lin, C.X.; Zhao, X.S.; Ismadji, S. *Journal of supercritical fluids* **2013**, *75*, 11-20.

[8] Muppaneni, T.; Reddy, HK.; Ponnusamy, S.; Patil, P.D.; Sun, Y.; Daily, P.; Deng, S. *Fuel* **2013**, *107*, 633-640.

[9] Marchitan, N.; Cojocaru, C.; Mereuta, A.; Duca, G.; Cretescu, I.; Gonta, M. *Seperation and Purification Technology* **2010**, *75*, 273-285.

[10] Xu, G.; Song, H.; Chen, P.; Fang, P.; Zhang, B. *Trans. CSAE* **2008**, *24*, 230-233.

[11] Rajendra, M.; Jena, P.C.; Raheman, H. *Fuel* **2009**, *88*, 868-875.

[12] Yuste, A.J.; Dorado, M.P. *Energy Fuel* **2006**, *20*, 399-402.

[13] Stamenkovic, O.S.; Rajkovic, K.; Milic, P.S.; Veljkovic, V.B. *Fuel Processing Technology* **2013**, *114*, 101-108.

[14] Rajkovic, K.M.; Avramovic, J.M.; Milic, P.S.; Stamenkovic, O.S.; Veljkovic, V. *Chemical Engineering Journal* **2013**, *215*, 82-89.

[15] Ramadhas, A.S.; Jayaraj, S.; Muraleedharan, C.; Padmakumari, K. *Renewable Energy* **2006**, *31*, 2524-2533.

[16] Rodríguez, R.P.; Borroto, Y.S.; Lapuerta, M.; Pérez, L.G.; Verhelst, S. *Energy Conversion and Management* **2013**, *65*, 255-261.

[17] Ying, Y.; Shao, P.; Jiang, S.; Sun, P. *IFIP* **2009**, *294*, 1239-1249.

[18] Basri, M.; Rahman, R.; Ebrahimpour, A.; Salleh, A.B.; Gunawan, E.R.; Rahman, M.B.A. *BMC Biotechnology* **2007**, *7*, 1 -14

[19] Moradi, G.R.; Dehghani, S.; Khosravian, F.; Arjmandzadeh, A. *Renewable Energy* **2013**, *50*, 915-920.

[20] Stamenkovic, O.S.; Velickovic, A.V.; Kostic, M.D.; Jokovic, N.M.; Rajkovic, K.; Milic, P.S.; Veljkovic, V.B. *Energy Conversion and Management* **2015**, *103*, 235-243.

[21] Betiku, E.; Ajala, S.O. *Industrial Crops and Products* **2014**, *53*, 314-322.

[22] Betiku, E.; Okunsolawo, S.S.; Ajala, S.O.; Odedele, O.S. *Renewable Energy* **2015**, *76*, 408-417.

[23] Betiku, E.; Omilakin, O.R.; Ajala, S.O.; Okeleye, A.A.; Taiwo, A.E.; Solomon, B. O. *Energy* **2014**, *72*, 266-273.

[24] Moorthi, N.S.V.; Franco, P.A.; Ramesh, K. *Journal of the Chinese Institute of Engineers* **2015**, *38*, 731-741.

[25] Maran, J.P.; Priya, B. *Ultrasound Sonochemistry* **2015**, *23*, 192-200.

[26] Maran, J.P.; Priya, B. *Fuel* **2015**, *143*, 262-267.

[27] Sarve, A.; Sonawane, S.S.; Varma, M.N. *Ultrasound Sonochemistry* **2015**, *26*, 218-228.

[28] Chakraborty, R.; Sahu, H. *Applied energy* **2014**, *114*, 827-836.

[29] ISO-660. Animal and vegetable fats and oils. Determination of acid value and acidity.; Geneva, ISO **1983**.

[30] Varma, M.N.; Madras, G. *Industrial Engineering & Chemistry Research* **2007**, *46*, 1-6.

[31] Shi, X.; Jin, D.; Sun, Q.; Li, W. *Renewable Energy* **2010**, *35*, 1493-1498.

[32] Gadhe, A.; Sonawane, S.; Varma, M.N. *International journal of hydrogen energy* **2013**, *38*, 6607-6617.

[33] Akintunde, A.M.; Ajala, S.O.; Betiku, E. *Industrial Crops and Products* **2015**, *67*, 387-394.

[34] Betiku, E.; Okunsolawo, S.S.; Ajala, S.O.; Odedele, O.S. *Renewable Energy* **2015**, *76*, 408-417.

[35] Betiku, E.; Omilakin, O.R.; Ajala, S.O.; Okeleye, A.A.; Taiwo, A.E.; Solomon, B. O. *Energy* **2014**, *72*, 266-273.

[36] Moorthi, N.S.V.; Franco, P.A.; Ramesh, K. *Journal of the Chinese Institute of Engineers* **2015**, *38*, 731-741.

[37] Garson, G.D. *AI expert* **1991**, *6*, 46-51.

[38] Shin, H.Y.; Lim, S.M.; Bae, S.Y.; Oh, S.C. *Journal of Analytical and Applied Pyrolysis* **2011**, *92*, 332-338.

[39] Imahara, H.; Minami, E.; Hari, S.; Saka, S. *Fuel* **2008**, *87*, 1-6.

[40] Patil, P.D.; Gude, V.G.; Mannarswamy, A.; Deng, S.; McGee, S.M.; Rhodes, I.; Lammers, P.; Nirmalakhandan, N.; Cooke, P. *Bioresource Technology* **2011**, *102*, 118-122.

[41] Anitescu, G.; Bruno, T.J. *Journal of Supercritical Fluid* **2012**, *63*, 133-149.

[42] Attanatho, L.; Magmee, S.; Jenvanitpanjakul, P. The joint international conference on sustainable energy and environment (SEE). Hua Hin.; Thailand; **2004**.

[43] He, H.; Wang, T.; Zhu, S. *Fuel* **2007**, *86*, 442-447.

[44] Balat, M. *Energy Sources.; Part A, Recovery* **2008**, *30*, 429-440.

[45] Vieitez, I.; Silva, C.; Alckmin, I.; Borges, G.R.; Corazza, F.; Oliveira, J.V.; Grompone, M.A.; Jachmanián, I. *Energy & Fuels* **2008**, *23*, 558-563.

[46] Han, H.; Cao, W.; Zhang, J. *Process Biochemistry* **2005**, *40*, 3148-3151.

[47] Yin, J.Z.; Xiao, M.; Song, J.B. *Energy Conversion and Management* **2007**, *49*, 908-912.

[48] Tsai, Y.T.; Lin, H.; Lee, M.J. *Bioresource Technology* **2013**, *145*, 362-369.

[49] Elmolla, E.S.; Chaudhari, M.; Eltoukhy, M.M. *Journal of Hazardous materials* **2010**, *179*, 127-134.

[50] Slokar, Y.M.; Zupan, J.; Marechal, A.M.L. *Dyes and Pigments* **1999**, *42*, 123-135.

[51] Shanmugaprakash, M.; Sivakumar, V. *Bioresource Technology* **2013**, *148*, 550-559.

Tables:

Table 1. CCD matrix of four independent variables along with experimental and predicted response

Temperature (^{o} C)	Molar ratio	Reaction Time (min.)	Initial CO_2 pressure (bar)	FAEE content (%)		
				Experimental	RSM	ANN
275	20:1	20	20	48.48	47.24	48.48
325	20:1	20	20	51.79	52.27	52.29
275	30:1	20	20	53.04	50.35	53.04
325	30:1	20	20	67.71	63.4	67.71
275	20:1	40	20	66.59	66.57	66.59
325	20:1	40	20	65.91	65.76	65.91
275	30:1	40	20	73.84	70.03	74.04
325	30:1	40	20	79.12	77.23	79.13
275	20:1	20	40	49.14	49.31	48.85
325	20:1	20	40	53.44	54.19	53.69
275	30:1	20	40	59.69	56.78	59.69
325	30:1	20	40	71.37	69.67	71.37
275	20:1	40	40	67.25	68.5	67.24
325	20:1	40	40	66.57	67.54	66.39
275	30:1	40	40	78.5	76.31	78.5
325	30:1	40	40	85.18	83.37	85.18
250	25:1	30	30	28.12	31.46	28.55
350	25:1	30	30	42.11	43.55	42.28
300	15:1	30	30	65.62	62.12	65.63
300	35:1	30	30	72.79	81.06	72.79
300	25:1	10	30	40.41	43.75	40.4
300	25:1	50	30	75.34	76.78	75.35
300	25:1	30	10	76.74	81.17	76.94
300	25:1	30	50	89.03	89.38	89.44
300	25:1	30	30	88.56	87.82	87.46
300	25:1	30	30	86.32	87.82	87.46
300	25:1	30	30	88.59	87.82	87.46

Table 2. Analysis of Variance (ANOVA) for the fitted polynomial quadratic model of FAEE content

Source	Sum of Squares	df	Mean Square	F Value	p-value Prob > F	
Model	6620.61	14	472.9	28.5929	< 0.0001	significant
A:Catalyst Concentration	219.252	1	219.252	13.2566	0.0034	
B:Methanol/oil molar ratio	537.896	1	537.896	32.5227	< 0.0001	
C:Temperature	1636.14	1	1636.14	98.9258	< 0.0001	
D:time	101.024	1	101.024	6.1082	0.0294	
AB	64.2402	1	64.2402	3.88415	0.0723	
AC	34.1056	1	34.1056	2.06212	0.1766	
AD	0.0225	1	0.0225	0.00136	0.9712	
BC	0.1156	1	0.1156	0.00699	0.9348	
BD	18.9225	1	18.9225	1.14411	0.3058	
CD	0.02103	1	0.02103	0.00127	0.9721	
A^2	3376.25	1	3376.25	204.138	< 0.0001	
B^2	351.253	1	351.253	21.2378	0.0006	
C^2	1012.8	1	1012.8	61.2367	< 0.0001	
D^2	8.67567	1	8.67567	0.52456	0.4828	
Residual	198.469	12	16.5391			
Lack of Fit	195.079	10	19.5079	11.5075	0.0825	not significan
Pure Error	3.39047	2	1.69523			
Cor Total	6819.07	26				
R^2 = 0.9709	**Adj. R^2 = 0.9369**		**Pred. R^2 = 0.8341**	**CV = 6.13**	**S = 4.07**	

Table 3. Comparison of 10 backpropagation (BP) algorithm with 10 neurons in hidden layer

Backpropagation (BP) algorithms	Function	Mean squared error (MSE)	Iteration number	Correlation coefficient (R^2)	Best linear equation
Resilient backpropagation	trainrp	6.5245	35	0.981	y = 0.983x + 0.240
Fletcher-Reeves conjugate gradient backpropagation	traincgf	0.8231	64	0.927	y = 0.962x + 2.325
Polak-Ribiere conjugate gradient backpropagation	traincgp	0.00017	48	0.999	y = 0.994x + 0.409
Powell-Beale conjugate gradient backpropagation	traincgb	0.5166	26	0.979	y = 0.978x + 1.384
Levenberg-Marquardt backpropagation	trainlm	0.00527	15	0.998	y = 0.992x + 0.403
Scaled conjugate gradient backpropagation	trainscg	0.06355	63	0.989	y = 0.989x + 0.791
BFGS quasi-Newton backpropagation	trainbfg	0.0272	10	0.998	y = 0.998x + 0.174
One step secant backpropagation	trainoss	0.4323	103	0.977	y = 0.985x + 1.117
Variable learning rate backpropagation	traingdx	0.0667	55	0.976	y = 0.979x + 1.425
Gradient Descent with adaptive learning rate	traingda	0.0886	73	0.980	y = 0.987x + 1.704

Table 4a. Matrix of weights, W_1: weights between input and hidden layers; W_2: weights between hidden and output layers

W_1						W_2	
Neuron	**Variable**				**Bias**	**Neuron**	**Weight**
	Temp.	**Molar ratio**	**Time**	**CO_2 pressure**			
1	0.44089	-0.302	1.3715	-1.6845	-2.7861	1	-0.18261
2	1.6029	-1.8237	1.0114	0.12937	-1.7488	2	-0.55982
3	1.6085	1.2886	-1.2555	0.08211	-2.0685	3	1.2491
4	-1.4374	0.36731	-1.9491	-0.238	1.2039	4	0.03047
5	-0.433	-1.4371	0.83634	1.3732	-1.0401	5	-0.09378
6	2.6774	1.5293	-2.2877	-0.1141	-1.5536	6	-1.1185
7	2.3905	0.1609	-0.6757	1.2321	0.52144	7	0.35442
8	2.1526	0.28323	1.0811	-0.1826	1.8328	8	1.194
9	0.15168	0.14845	0.55727	1.6455	2.8863	9	-0.40243
10	-0.7973	-0.333	1.22	1.469	-3.0539	10	0.22069
						Bias	-0.35551

Table 4b. Relative importance of input variables on the output variable

Input variable	**% Importance**
Temperature	39.24
Methanol/oil molar ratio	19.61
Reaction time	28.57
Initial CO_2 pressure	12.58
Total	100.00

Table 5. Unseen validation data set for developed model

Sr. No.	Temperature (^{o}C)	Molar ratio (v/v)	Reaction Time (min)	CO_2 pressure (bar)	FAEE content (%)		
					Experimental	RSM	ANN
1.	275	25	20	40	54.38	57.1	56.37
2.	325	25	40	20	78.12	75.55	79.66
3.	300	30	30	30	86.5	88.5	84.11
4.	300	20	40	40	71.43	80.6	75.48
5.	275	30	35	40	72.16	76.59	77.65
6.	325	30	35	40	69.54	85.11	76.66

Table 6. Comparison between predictive capabilities of RSM and ANN models

Performance parameters	**DoE data**		**Validation data**	
	RSM	**ANN**	**RSM**	**ANN**
Correlation coefficient (R^2)	0.971	0.999	0.658	0.868
Root mean square Error (RMSE)	2.711	0.416	7.691	4.185
Standard predicted deviation (SEP %)	4.087	0.627	10.67	5.81
Absolute average deviation (AAD %)	3.398	0.338	8.574	5.239

Table 7. Fuel properties of Mahua oil, Mahua oil biodiesel, Diesel, ASTM and DIN EN 14214

Sr. No.	Properties		Mahua oil	Mahua oil Biodiesel	Diesel	ASTM standard D-6751	DIN-EN 14214
1.	Density at 15 ^{o}C	(Kg/L)	0.954	0.871	0.846	-	0.86-0.9
2.	Viscosity at 40 ^{o}C	(mm^2/s)	43.8	4.6	2.68	1.9-6.0	3.5-5.0
3.	Flash Point	(^{o}C)	231	186	70	>130	>120
4.	Fire Point	(^{o}C)	239	197	76		
5.	Pour Point	(^{o}C)	15	3	-20	-	-
6.	Acid value	(mg of KOH/g)	38	0.29	-	<0.8	<0.5
7.	Calorific value	(MJ/Kg)	36	41	42.96	-	-
8.	Cetane number		48.57	50	47	Min. 47	Min. 51
9.	Cloud Point	(^{o}C)	1	3	-13	-	-
10.	Water content	volume%	1.32	0.017	0.02	Max. 0.05	Max. 0.05
11.	Carbon Residue	Mass %	0.57	0.21	0.17	Max. 0.05	Max. 0.05
12.	Sulphur	Wt %	-	< 0.005	0.001	Max. 0.05	Max. 0.05
13.	Total Glycerin	ppm	-	47	-	-	-

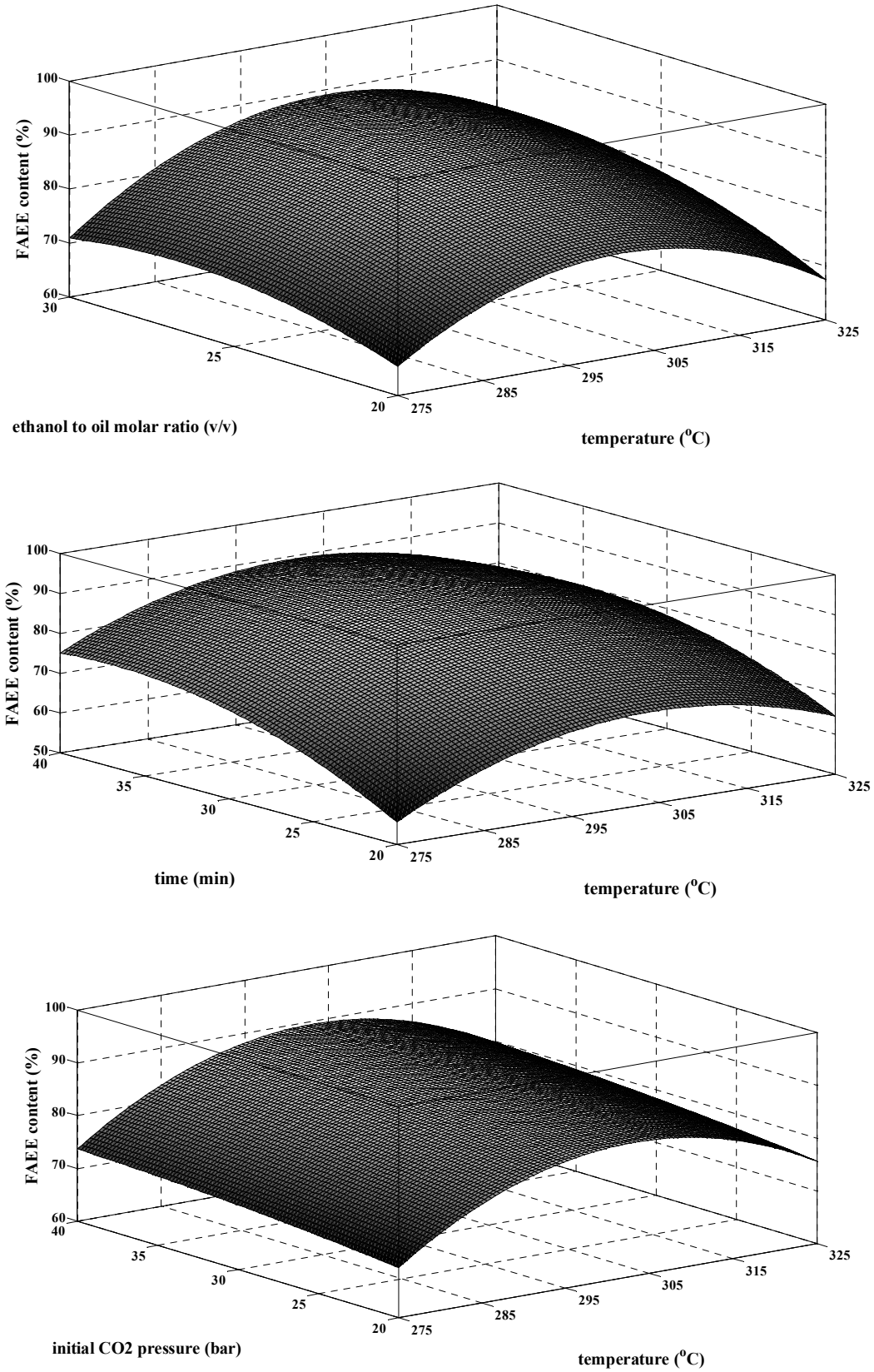

Figure 1. 3D response surface plots showing the relative effect of process variables on FAEE content (%) **(a)** effect of temperature and ethanol/oil molar ratio; **(b)** effect of temperature and reaction time; **(c)** effect of temperature and initial CO_2 pressure

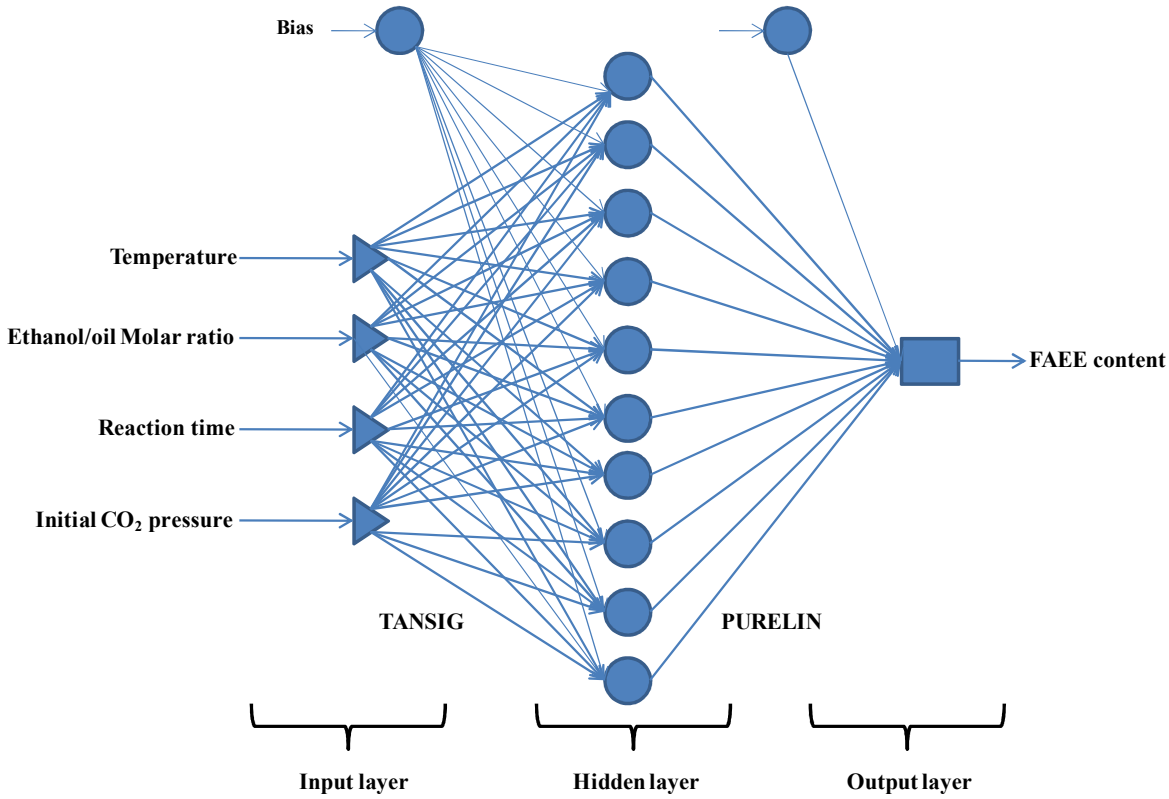

Fig. 2. Typical architecture of ANN with three layers

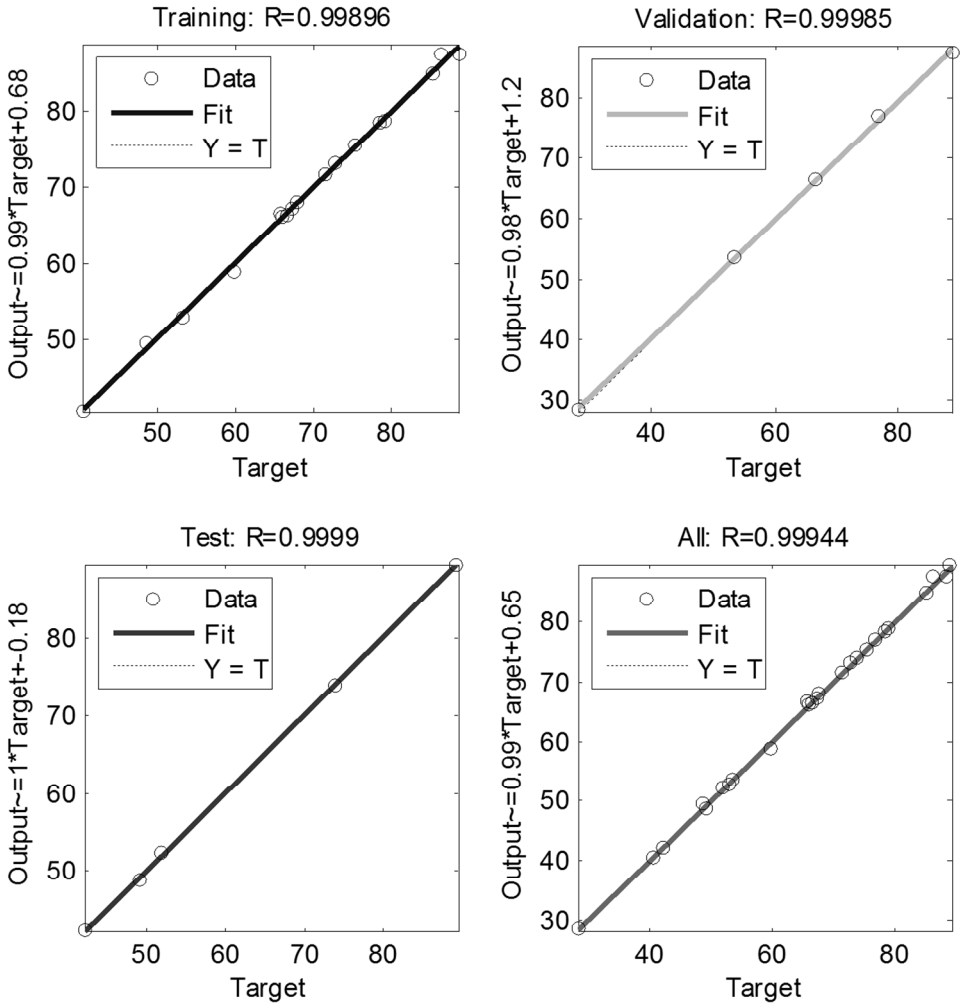

Fig. 3. Neural Network model with training, validation, test and all prediction set

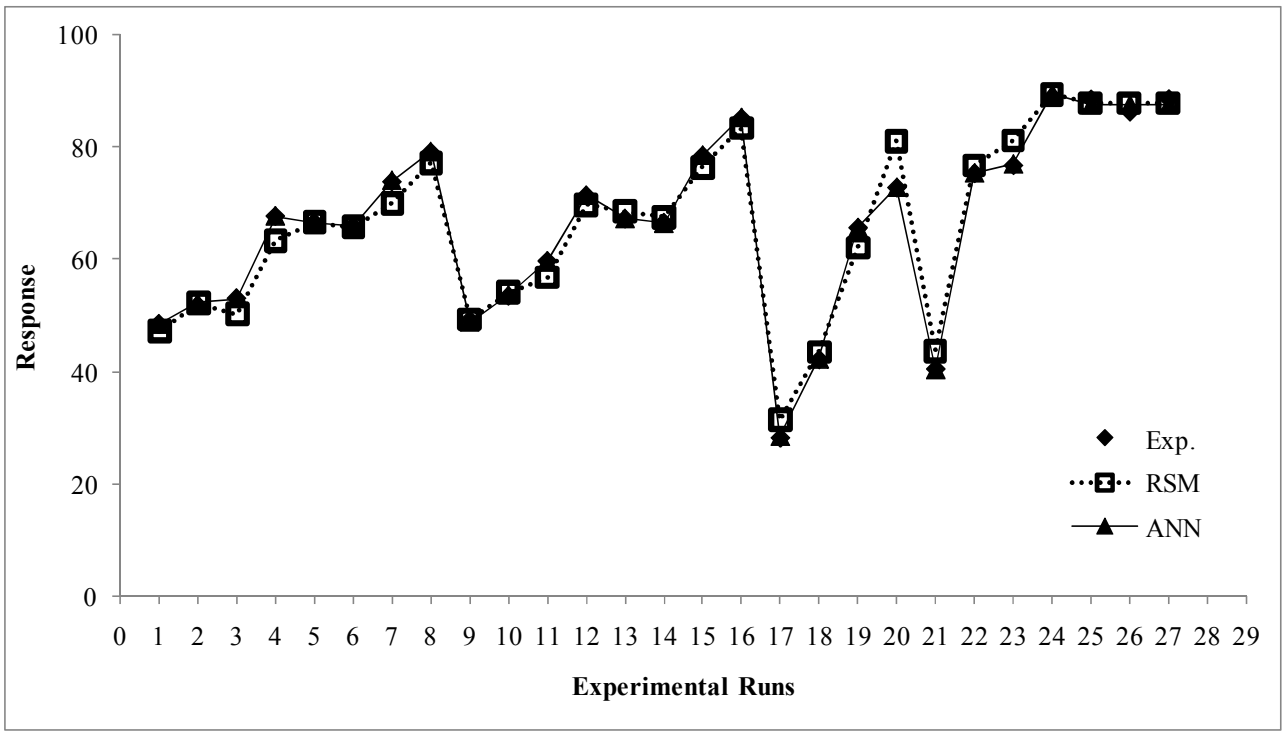

Fig. 4. Comparison between experimental and predicted values by RSM and ANN for each experimental run to obtained the FAEE content